A Novel Dual-Band Conformal Surface Plasmons Waveguide With Tunable Frequency Response In Large-scale

Yijiao Fang (03000133@wxc.edu.cn)
West Anhui University https://orcid.org/0000-0002-9297-6830
Jiangwei Zhong
Lenovo Research Shanghai Branch

Research Article

Keywords: Materials, Metamaterials, Surface plasmons, Electromagnetic waveguides

Posted Date: July 9th, 2021

DOI: https://doi.org/10.21203/rs.3.rs-586718/v1

Abstract

A novel dual-band conformal surface plasmons (CSPs) waveguide is designed and well studied in this paper. In earlier researches, we have recognized that electromagnetic field of CSPs waveguide are always confined to a sub-wavelength area and have a strong potential to be applied in devices designing. However, almost all of the earlier CSP structures is mainly focus on the fundamental mode characteristics with only single resonance frequency. Here we propose a innovative dual inverted-L structure with excellent performance not only on the fundamental mode but also on a new upper mode. This structure operates in microwave frequencies regime and shows outstanding frequency tunability characteristic. Being different from frequency characteristics in the earlier CSP waveguides which always used to be designed single-frequency device, dual-frequency tunability can be obtained via the dual L-type bending branch of the periodical CSP structure. In present paper, we also realize a tunable dual-frequency filter by changing the scaling factor of inverted-L stubs.

Introduction

Surface plasmons (SPs) are the surface electromagnetic waves(SEMs) inspired on the metal/dielectric interface in the optical frequencies [1]. Due to the excellent performance on intensively localized characteristic, electromagnetic field of the SPs waves can be localized around the metal/dielectric interfac within sub-wavelength scales. This unique characteristic have attracted much attention in recent years and shows the great potential and the broad prospect in the terahertz and microwave frequencies application. Therefore, a lot of efforts has been made to reduce the operating frequency of the SPs [2–4]. According to Drude Model, dielectric constant of metal depends on the plasma resonance frequency and exhibits perfect electrical conductor (PEC) properties in the microwave frequencies range. Electromagnetic field cannot be exist in PEC and then SPs also cannot be supported on smooth PEC surfaces. However, by corrugating the smooth metal surfaces with periodic subwavelength structures, a novel surface mode called as spoof SPs could also be supported on metal surfaces in the microwave frequencies range. Spoof SPs have similar characteristics to the traditional SPs and make the high-field confined microwave circuits and components possible to be fabricated [5–7].

More recently, a ultra-thin and flexible spoof SPs, which is called as conformal SPs (CSPs), has been proposed and offers a big step forward in developing and operating ultra-compact integrated microwave circuits[8–13]. This proposed CSPs structure is based on a ultra-thin metal microstrip line decorated by periodically grooves surface. According to the design guideline above, several kinds of CSPs devices have been designed and different approaches to controll the dispersion characteristics of the CSPs have also been investigated [14–18]. Naturally, most of research efforts, such as U-shaped, T-shaped, hole arrays or other symmetric/asymmetric CSP structure, are mainly directed towards design and application in fundamental mode of the CSPs waveguide[19–25]. As mentioned in earlier studies, the second-order mode is existed in traditional CSP geometries, nevertheless, the theoretical and experimental results show that the resonant frequency (or so-called cutoff frequency) of second-order mode is almost twice as much as that of fundamental mode. Since the ratio of these two resonant frequencies is an almost

constant value and the comparative magnitudes of these two values is difficult to modulate, the adaptability and practicality of second-order mode would be limited.

In this paper, a dual-band conformal surface plasmons waveguide is proposed to achieve sufficiently small and tunable frequency interval between fundamental mode and second-order mode. This proposed waveguide has a periodic array of two parallel inverted-L sleeves at the upper side of a metal stripe. We investigate the dispersion curves of this new geometry and the frequency-tunable property by changing the length of each inverted-L sleeve. We also compare the electromagnetic field distribution of these two modes. We investigate the properties of this waveguide by using finitedifference time-domain FDTD simulations with CST STUDIO SUITE. Details of the waveguide design and simulational results are displayed and analysed in the following. A dual-frequency filter device based on this theory are also shown in this paper.

Model Construction And Result Analysis

The schematic representation of the novel dual inverted-L CSPs waveguide is shown in Fig. 1(a) in this paper. One unit cell of this periodical structure consists of a metal stripe with subwavelength double inverted-L stubs and an lossy FR4 dielectric substrate, where L_1 is the length of the upper inverted-L branch, and L_2 is the length of the lower inverted-L branch, h_1 and h_2 are the height of these two inverted-L geometries respectively, w is the width and d is a period of the waveguide. All geometric parameters of the waveguide are listed in Table I. Unlike other periodic CSPs waveguides in early research, the proposed CSPs waveguide has a more complex structure to achieve an additional upper mode. This newly increased second-order mode comes from electromagnetic-field coupling between the parallel stub structure and the long stripe which we treat as a metal ground plane. We will analyze the details of frequency response with the full-wave simulated results in the following.

Table I GEOMETRICAL PARAMETERS OF PROPOSED (The unit of all the parameters is mm.)

d	L_1	L_2	a	b
5	3.7	3.4	0.1	0.1
h_1	h_2	w	t_1	t_2
0.5	0.8	0.7	0.02	0.1

The dispersion curves of a conventional model and this novel dual-band CSPs waveguide (Prototype single inverted-L and Proposed dual inverted-L) are presented by blue curves and red curves in Fig. 2 respectively. Black curve represents the light momentum in free space. The inset in Fig. 2 displays one unit cell of the contrasting single inverted-L prototype, which has the same dimensions as the dual inverted-L one besides the lack of the lower one of the stubs. As depicted in the figure, we can note that the impedance bandwidth in the proposed model are significant smaller than that in single inverted-L model. For the single inverted-L one, the resonant frequencies is located at 14GHz and 30GHz

corresponding to the fundamental mode and the second order mode respectively. Apparently the second resonant frequency is twice as much as the fundamental one. The fundamental resonant frequency value in the dual inverted-L structure is 14.2GHz which is pretty close to that in the single inverted-L structure. However, the second resonant frequency value is around 16GHz. which is significantly lower than that in the single inverted-L structure. This feature makes dual-band RF devices can be designed on the adjacent frequencies. Also note that the second mode of single inverted-L model is on the left region of the free space light line in Fig. 2. It means that it's a radiated mode and different from the others, in which the electromagnetic field will radiate to the free space instead of being restrained around the waveguide.

Figure 3(a) shows the surface current density distributions of the two lowest modes in the proposed waveguide, which is propagating along the dual inverted-L stub and excited at 14.2GHz (the left column in Fig. 3) and 16GHz (the right column in Fig. 3) respectively. Black arrows are used to represent the direction and magnitude of the surface current. Obviously, the excitation of these two modes correspond to the relative surface current direction between the stubs and the ground plane. We can see that, for the fundamental mode, the surface current of the upper inverted-L stub move in the opposite direction of the ground plane. In contrast to the first situation, for the second order mode, the surface current of the lower inverted-L stub move in the opposite direction of the ground plane.

According to the analysis above, the dual inverted-L structure generate a new kind of resonance mode with a cutoff frequency of 16GHz at higher frequency due to the reverse surface current direction between the lower inverted-L stub and the ground plane.

In order to further verify the mechanism responsible for the new higer resonance mode, the simulation results of electric field and magnetic field distributions are also presented in Fig. 3. The veracity of the result analyzed above can be confirmed by comparison with the field distributing characteristics of these two modes. In Fig. 3(b) and (c), it can be seen that electric field mainly comes from the interaction of the positive and negative charges collected at the end of stubs and mirror image of ground plane respectively, which all due to the motion of reverse surface current.

Another particular feature of this dual inverted-L CSPs waveguide is frequency tunability characteristic. We consider the dual inverted-L stub structure with a varying constant L_1 and an invariant constant L_2. Figure 4 gives the dispersion curves with different length of L_2, which is varying from 3.4 mm to 3.8 mm with equal step 0.2 mm. The results show that, as the length L_2 increases, the resonant frequency of the second order mode falloff significantly and move gradually towards the fundamental resonant frequency. Further analysis reveals that this second order mode is suppressed in the waveguide when its resonant frequency is close to or even below the fundamental one. Thus, for the present parameters, this second order resonant frequency can be tuned in the range of 16 to 14.8GHz. It is well suited for dual-band RF devices designing with flexible operating frequency selection in large-scale. In addition, unlike second order resonant frequency, the fundamental resonant frequency are almost disassociated with the parameter L_2.

By using this design methodology, a dual-band bandpass filter device is presented and discussed in Fig. 5. The proposed filter is composed of a coplanar waveguide and a dual inverted-L structure array. The dual inverted-L structure has the same schematic configration and periodicity as it has in Fig. 1. The width of the narrow input port is t_2 and a tapered section is adopted to match the impedance between the narrow input and the main part of the filter. We present the results of reflection coefficient S11 of the proposed filter in Fig. 5(b) with t_3 = 0.3mm, t_4 = 1.8mmand w = 0.7mm. We can see that in the 14.2GHz band S11 is below 0.6 dB, meanwhile, in the 16.2GHz band S11 is below 1 dB. We can find from Fig. 5(b) that the frequency interval between these two pass band can be tuned in a wide range. The second-band shift from 16.2GHz to 15GHz as the parameter L_2 increased from 3.4mm (blue curve) to 3.8mm (red curve). By contrast, the position of first-band is almost immovable. Bandpass frequency selectivity of such filter correspond exactly to resonant frequencies of the proposed waveguide in Fig. 4. The results shows that strong operability and high flexibility can be achieved by utilized this methodology for device designing.

Conclusion

In this paper, we have demonstrated that a novel dual inverted-L CSPs waveguide can support a new upper mode and achieve much lower frequency interval between the fundamental mode and the upper mode. With an varying structural parameters of lower inverted-L strip, the proposed waveguide can provides a more flexible and changeable frequency interval than that of a conventional CSPs waveguide. By using this feature, we also realize a dual-band bandpass filter whose frequency selection characteristic can be controlled by the geometry parameters.

Declarations

Acknowledgments

This work is supported by the Fundamental Research Funds of West Anhui University under Grant Nos. WGKQ2021010.

Funding: the Fundamental Research Funds of West Anhui University under Grant Nos. WGKQ2021010

Conflicts of interest/Competing interests: Not applicable

Availability of data and material: The data used in this study is available from the corresponding author on reasonable request.

Code availability: Not applicable

Authors' contributions: Yijiao Fang contributed to the conception and data analyses of the study. Yijiao Fang is the corresponding author and also the first author. Jiangwei Zhong contributed to the constructive discussions of the study. Jiangwei Zhong is the second author.

Ethics approval: Not applicable

Consent to participate: Not applicable

Consent for publication: Written informed consent for publication was obtained from all participants.

References

1. Barnes WL, Dereux A, Ebbesen TW *(*2003*)* Surface plasmon subwavelength optics, Nature, 424(6950): 824–830. https://doi.org/10.1038/nature01937
2. Pendry JB *(*2004*) Mimicking Surface Plasmons with Structured Surfaces*, *Science*, *305*(*5685*): *847–848*. https://doi.org/10.1126/science.1098999
3. Garcia-Vidal FJ, L Martín-Moreno, Pendry JB *(*2005*)* Surfaces with holes in them: New plasmonic metamaterials, Journal of Optics A Pure Applied Optics, 7(2): S97. https://doi.org/10.1088/1464-4258/7/2/013
4. Hibbins AP (2005) Experimental Verification of Designer Surface Plasmons. Science 308(5722):670–672. https://doi.org/10.1126/science.1109043
5. Nahata A, Cui A, Kumar G *et al (*2011*)* Planar terahertz waveguides based on complementary split ring resonators, Opt Express, 19(2):1072–1080. https://doi.org/10.1364/OE.19.001072
6. Miguel Navarro-Cía, Beruete M, Sorolla M *et al (*2011*)* Enhancing the Dual-Band Guiding Capabilities of Coaxial Spoof Plasmons via use of Transmission Line Concepts, Plasmonics, 6(2):295–299. https://doi.org/10.1007/s11468-011-9203-x
7. Maier SA, Andrews S R, Martín-Moreno L *et al (*2006*)* Terahertz Surface Plasmon-Polariton Propagation and Focusing on Periodically Corrugated Metal Wires, Phys Rev Lett, 97(17):176805. https://doi.org/10.1103/PhysRevLett.97.176805
8. Fernandezdominguez AI, Garciavidal F J, Martincano D *et al (*2010*)* Domino plasmons for subwavelength terahertz circuitry, Opt Express, 18(2):754. https://doi.org/10.1364/OE.18.000754
9. Ma Y, Zhou J, Wang Z *(*2010*)* Surface Plasmon Waves on Structured Metal Surface With Periodic Grooves Modified by Perpendicular Cuts, IEEE Photonics Technol Lett, 22(7):450–452. https://doi.org/10.1109/LPT.2010.2040987
10. Hooper IR, Tremain B, Dockrey JA *et al (*2014*)* Massively Sub-wavelength Guiding of Electromagnetic Waves, Sci Rep, 4:7495. https://doi.org/10.1038/srep07495
11. Gao X, Hui Shi J, Shen X *et al (*2013*)* Ultrathin dual-band surface plasmonic polariton waveguide and frequency splitter in microwave frequencies, Appl Phys Lett, 102(15):824. https://doi.org/10.1063/1.4802739
12. Liao Z, Zhao J, Pan BC *et al (*2014*)* Broadband transition between microstrip line and conformal surface plasmon waveguide, J Phys D: Appl Phys, 47(31):315103. https://doi.org/10.1088/0022-3727/47/31/315103

13. Ma HF, Shen X, Cheng Q *et al (*2014*)* Broadband and high-efficiency conversion from guided waves to spoof surface plasmon polaritons, Laser Photonics Rev, 8(1):146–151. https://doi.org/10.1002/lpor.201300118
14. Zhang W, Zhu G, Sun L *et al (*2015*)* Trapping of surface plasmon wave through gradient corrugated strip with underlayer ground and manipulating its propagation, Appl Phys Lett, 106(2):021104. https://doi.org/10.1063/1.4905675
15. Liu L, Li Z, Xu B *et al (*2015*)* Dual-band trapping of spoof surface plasmon polaritons and negative group velocity realization through microstrip line with gradient holes, Appl Phys Lett, 107(20):847. https://doi.org/10.1063/1.4935976
16. Zhao S, Zhang H C, Zhao J *et al (*2017*)* An ultra-compact rejection filter based on spoof surface plasmon polaritons, Sci Rep, 7:10576. https://doi.org/10.1038/s41598-017-11332-8
17. Shen X, Cui T J *(*2013*)* Planar plasmonic metamaterial on a thin film with nearly zero thickness, Appl Phys Lett, 102(21):211909. https://doi.org/10.1063/1.4808350
18. Shen X, Cui T J, Martin-Cano D *et al (*2013*) Conformal surface plasmons propagating on ultrathin and flexible films, Proceedings of the National Academy of Sciences, 110(1): 40–45.* https://doi.org/10.1073/pnas.1210417110
19. Kianinejad A, Chen Z N, *and* Qiu CW *(*2018*)* Full Modeling, Loss Reduction, and Mutual Coupling Control of Spoof Surface Plasmon-Based Meander Slow Wave Transmission Lines, IEEE Trans Microw Theory Tech, 66(8):3764–3772. https://doi.org/10.1109/TMTT.2018.2841857
20. Liu XY, Feng Y J, B, Zhao *J M &* Jiang T *(*2016*)* Backward spoof surface wave in plasmonic metamaterial of ultrathin metallic structure, Sci Rep, 6:20448. https://doi.org/10.1038/srep20448
21. Liang Y, Yu H, J C, AnakAgungAlitApriyana, Li N, Y&Sun L L *(*2016*)* On-chip sub-terahertz surface plasmon polariton transmission lines with mode converter in CMOS, Sci Rep, 6:30063. https://doi.org/10.1038/srep14853
22. Aghadjani M, Mazumder P *(*2015*)* THz Polarizer Controller Based on Cylindrical Spoof Surface Plasmon Polariton (C-SSPP), IEEE Transactions on Terahertz Science Technology 5(4):556–563. https://doi.org/10.1109/TTHZ.2015.2439677
23. Aghadjani M, Erementchouk M, Mazumder P *(*2016*)* Spoof Surface Plasmon Polariton Beam Splitter, IEEE Transactions on Terahertz Science Technology PP(99). https://doi.org/10.1109/TTHZ.2016.2599289
24. Zhou YJ, Yang B J *(*2015*)* Planar spoof plasmonic ultra-wideband filter based on low-loss and compact terahertz waveguide corrugated with dumbbell grooves, Appl Opt, 14(54):4529–4533. https://doi.org/10.1364/AO.54.004529
25. Ye LF, Xiao Y F, Liu YH, Zhang L, Cai GX, Liu QH *(*2016*)* Strongly Confined Spoof Surface Plasmon Polaritons Waveguiding Enabled by Planar Staggered Plasmonic Waveguides, Sci Rep, 6:38528. https://doi.org/10.1038/srep38528

Figures

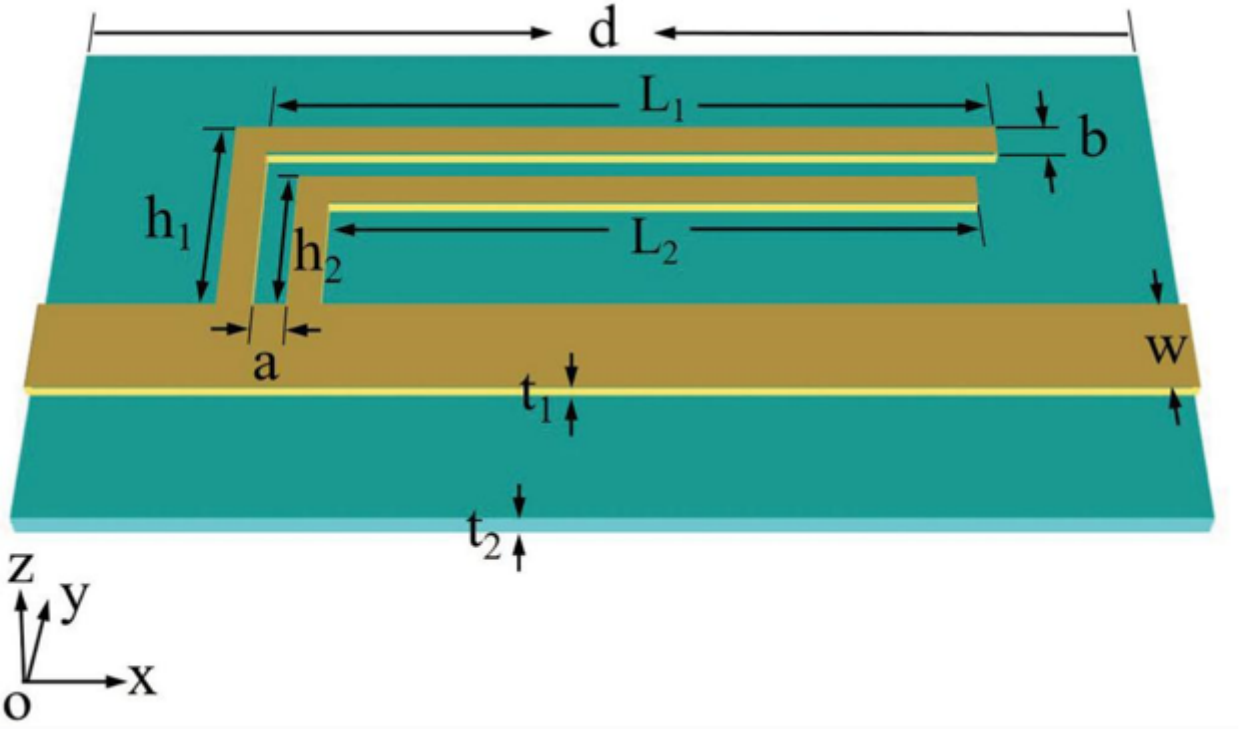

Figure 1

One unit cell element of the proposed dual inverted-L CSPs waveguide on lossy FR4 dielectric substrate.

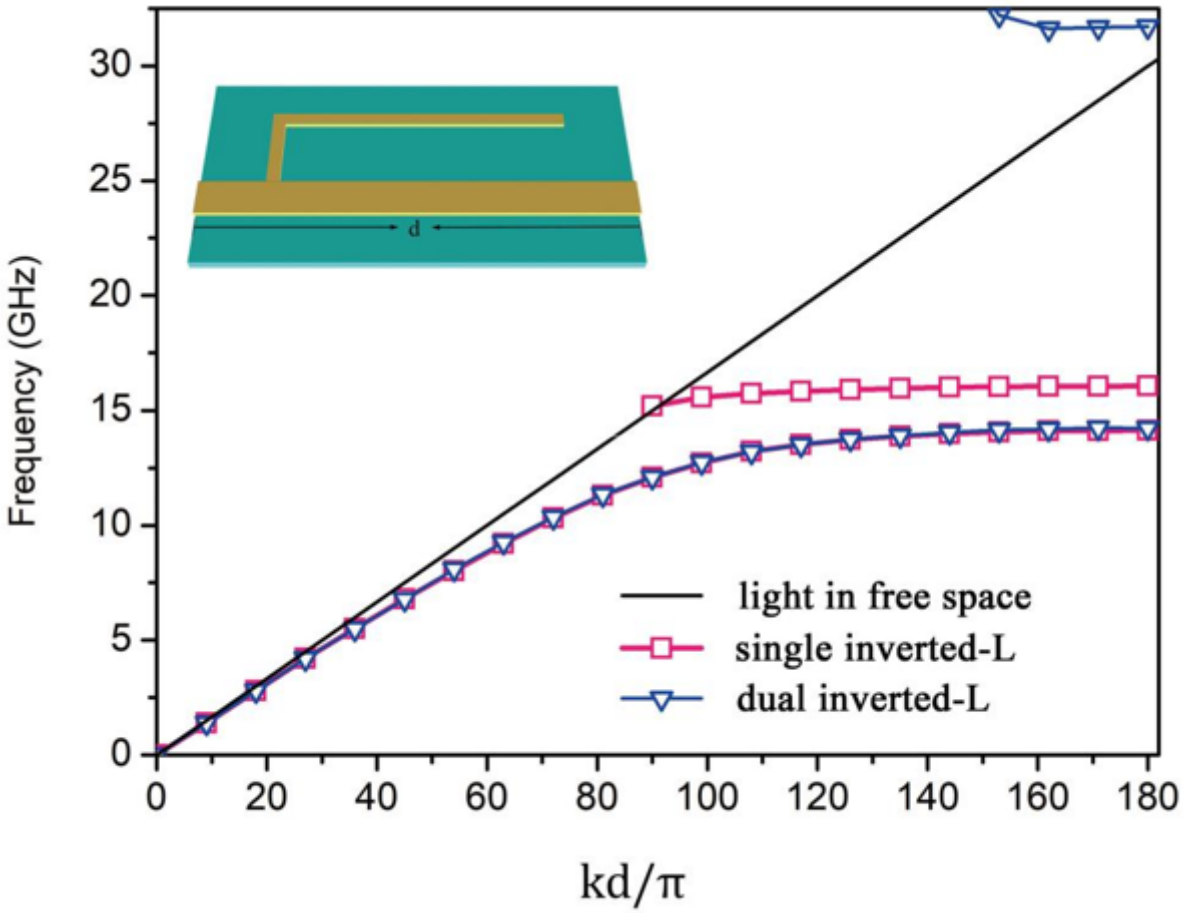

Figure 2

Dispersion curves of the fundamental and second mode for the single inverted-L and dual inverted-L CSPs waveguides, in which the blue line corresponds to the single inverted-L and the red line corresponds to the dual inverted-L structure.

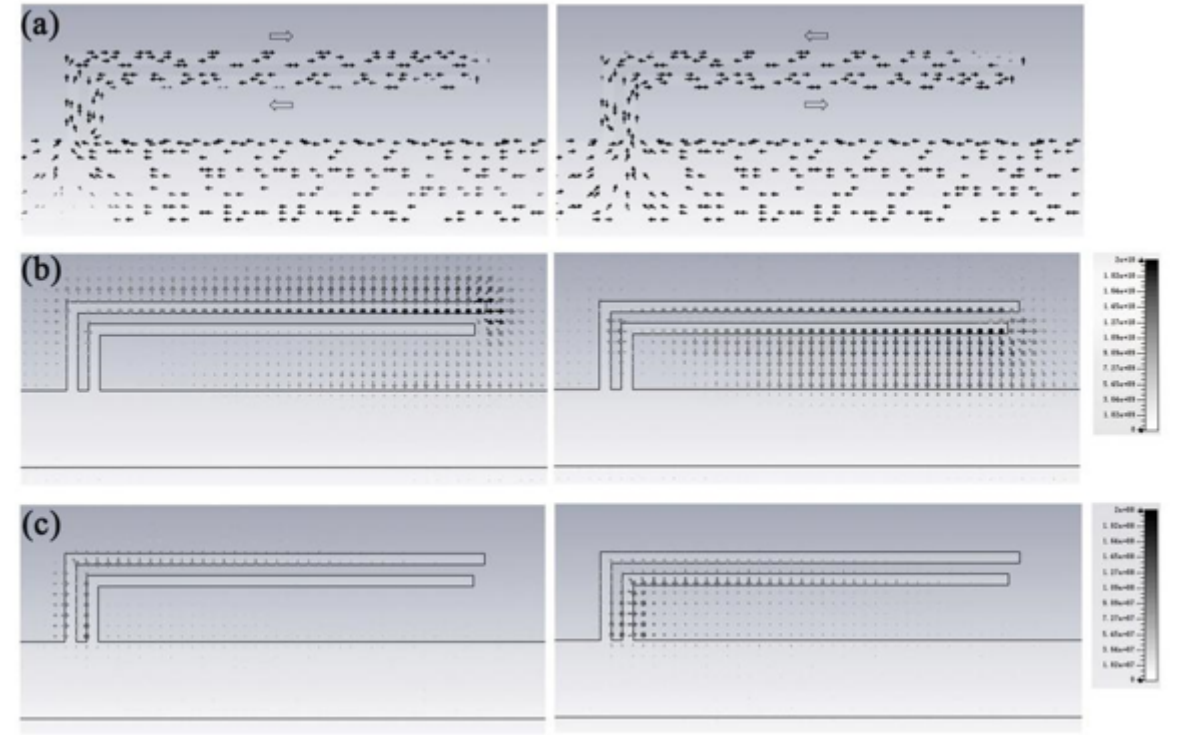

Figure 3

(a) surface current density, (b) magnetic field and (c) magnetic field distributions for the fundamental mode and the second-order mode at 14GHz (left) and 16GHz (right) respectively

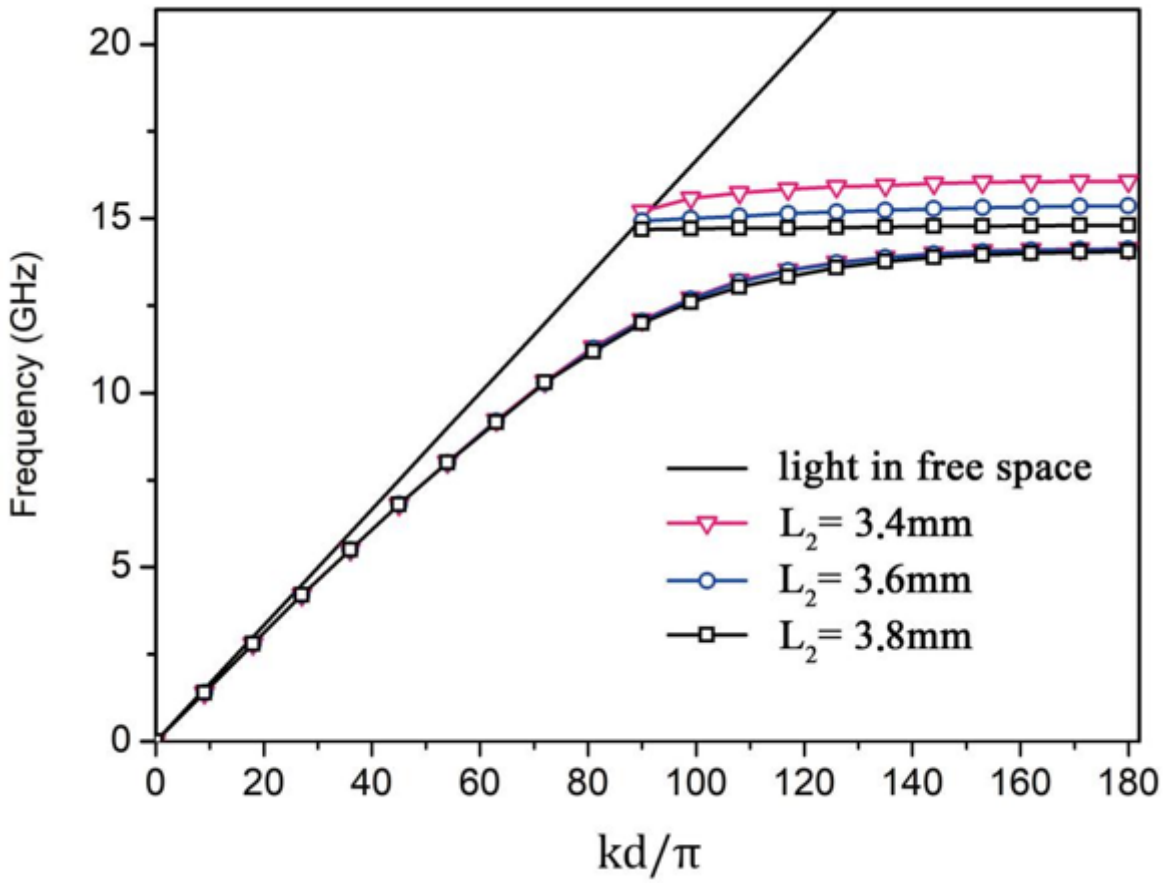

Figure 4

Dispersion curves for different lower inverted-L stub length L2= 3.4, 3.6, 3.8 mm.

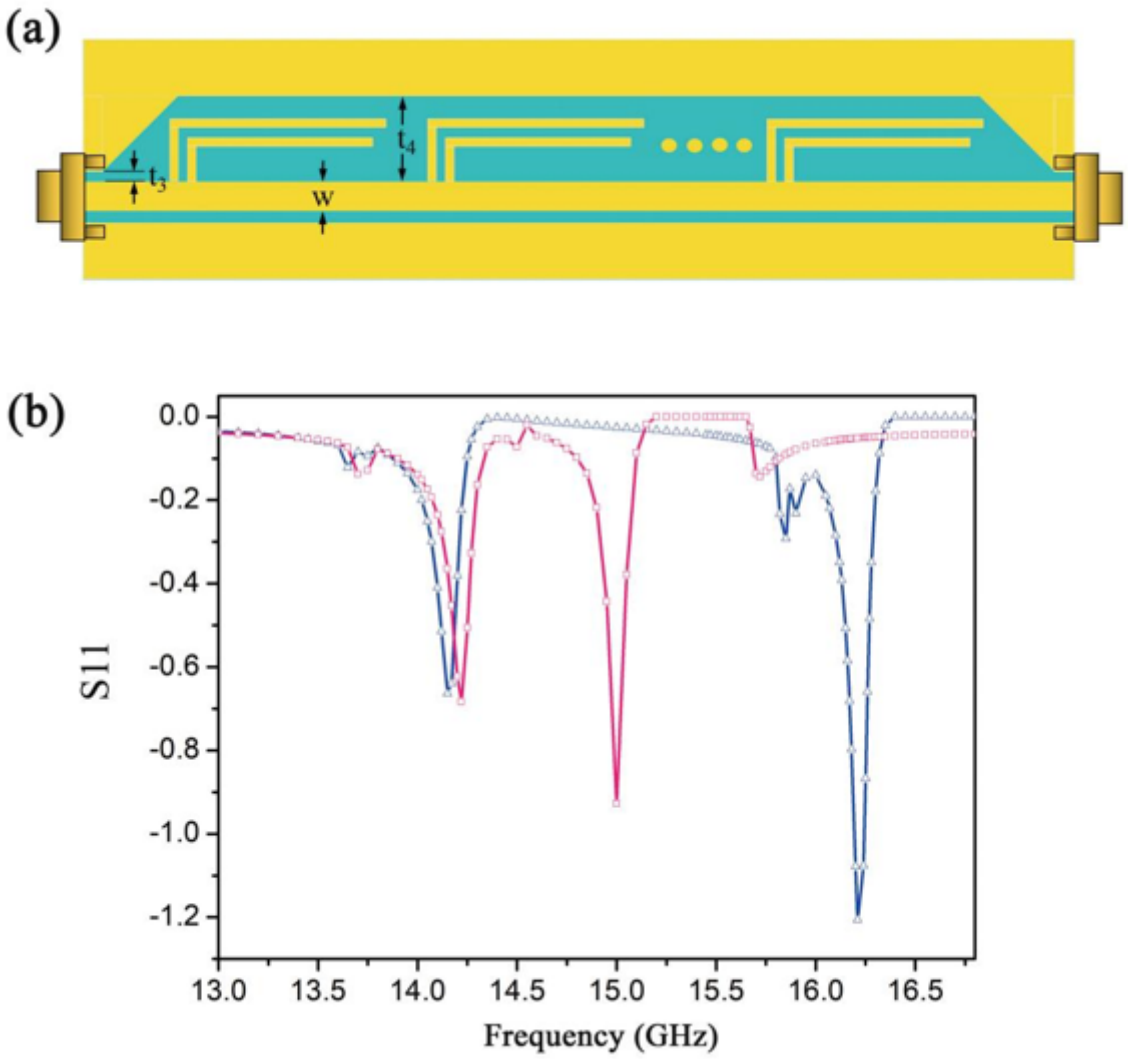

Figure 5

(a) Schematic configuration and (b) reflection coefficient S11 of the proposed spoof CSPs filter.